

# Phase Behavior and Selectivity of DNA-linked Nanoparticle Assemblies

D. B. Lukatsky and Daan Frenkel  
*FOM Institute for Atomic and Molecular Physics,  
 Kruislaan 407, 1098 SJ Amsterdam, The Netherlands*  
 (Dated: February 2, 2008)

We propose a model that can account for the experimentally observed phase behavior of DNA-nanoparticle assemblies (R. Jin et al., JACS **125**, 1643 (2003); T. A. Taton et al., Science **289**, 1757 (2000)). The binding of DNA-coated nano-particles by dissolved DNA linker can be described by exploiting an analogy with quantum particles obeying fractional statistics. In accordance with experimental findings, we predict that the phase-separation temperature of the nano-colloids increases with the DNA coverage of the colloidal surface. Upon the addition of salt, the demixing temperature increases logarithmically with the salt concentration. Our analysis suggests an experimental strategy to map *microscopic* DNA sequences onto the *macroscopic* phase behavior of the DNA-nanoparticle solutions. Such an approach should enhance the efficiency of methods to detect (single) mutations in specific DNA sequences.

PACS numbers:

Colloidal particles that can be selectively linked by specific sequences single-stranded DNA, represent an entirely novel class of complex liquids. With these particles, it becomes feasible to “design” multicomponent mixtures, where the attractive interaction between every pair of species can be controlled independently.

During the past few years, the unique molecular recognition properties of DNA have been exploited to create self-assembled nano-structures and nano-devices with a remarkable degree of control (see e.g. Ref. [1]). Self-assembled nanostructures based on DNA have also been utilized to detect specific DNA sequences [2, 3, 4, 5]. In nanoparticle-based DNA detection systems, single-stranded DNA (ssDNA) “probe” molecules are chemisorbed onto the surface of gold nanoparticles (Fig. 1). These probe ssDNA’s can specifically bind to a dissolved “target” ssDNA and thus detect its presence with high sensitivity and selectivity: at high enough concentration, the target ssDNA strands induces a sharp demixing transition [6] that leads to aggregation of the nanoparticles coated with the complementary “probe” strands. These aggregates can be easily detected by optical means.

The sensitivity of the nanoparticle-based DNA detection method is some two orders of magnitude higher than that of the corresponding fluorophore-based DNA-array scheme [3]. But, in addition, the method can be used to distinguish different DNA sequences that differ from each other by only a single base. The reason is that a single mismatch in the DNA sequence results in a significant change in the DNA-colloid demixing temperature. The fluorophore-based systems lack this level of selectivity [3].

In a recent paper, Jin et al. [4] have analyzed the dependence of the dissolution temperature (see note [6]) of DNA-linked nanoparticles on the DNA coverage density, the particle size, and the salt concentration. In the experiments [3, 4] short DNA molecules ( $\sim 20$ -base oligonucleotides) and small gold colloids ( $\sim 10 - 50$  nm) were used. The principal experimental findings are the follow-

ing: (i) The higher the ssDNA coverage density on the surface of colloids, the sharper the dissolution profiles, and the higher the dissolution temperature. (ii) The addition of salt stabilizes the aggregates. The dissolution temperature increases logarithmically with salt concentration. The higher the salt concentration, the larger the total fraction of DNA-nanoparticle aggregates.

Below, we propose an explanation for these experimental findings. We argue that the origin of the sharp phase-transition profiles is the *entropic cooperativity* of the DNA-nanoparticle network. Upon cooling, the system undergoes liquid-liquid phase separation. The dense “liquid” phase is strongly cross-linked and behaves as a solid gel.

We first consider a simple model for a binary mixture of DNA-coated colloids. Each colloidal species is covered with specific ssDNA molecules, in such a way that all possible pairs of colloids can be bound by three types of complementary ssDNA linkers: *viz.*, *AA*, *BB*, and *AB*.

For the sake of simplicity, we use a lattice model to analyze the phase behavior of this system. Colloids of type *A* and *B* can occupy the nodes of a three-dimensional lattice with coordination number *q*. The system is grand canonical with respect to all the components:  $\mu_A^c$  and  $\mu_B^c$  are the chemical potentials of colloids of species *A* and *B*, respectively; and  $\mu_{AA}$ ,  $\mu_{BB}$ , and  $\mu_{AB}$  are the corresponding chemical potentials of linkers. First, we consider the situation where only linkers of type *AB* are present (this corresponds to the experimental conditions of Refs. [3, 4]). For this system, the grand canonical partition function is:

$$Z = \sum_{N_A, N_B, n} g(N_A, N_B, n) Q_{AB}^n e^{\frac{\mu_A^c N_A + \mu_B^c N_B}{T}}, \quad (1)$$

where  $N_A$  and  $N_B$  are the number of colloids *A* and *B*, respectively, *n* is the number of nearest neighbor *AB* colloidal pairs for a given realization of the grand canonical ensemble, and  $g(N_A, N_B, n)$  is the total number of possi-

ble configurations with  $n$  nearest neighbor  $AB$  pairs for a given values of  $N_A$  and  $N_B$ . The sum with respect to  $n$  extends over all values of  $n$  consistent with the fact that there are  $N_A$  and  $N_B$  colloids  $A$  and  $B$  present. The number of links between a given pair of colloids depends on the surface density of probe strands on the  $A$  and  $B$  colloids. If there is only one pair of probe strands per contact, then this pair can accommodate at most one linker and the bound linkers obey Fermi-Dirac statistics. In contrast, when there are (infinitely) many probe strands per contact, then the binding of linkers is determined by Bose-Einstein statistics [7]. In general, the maximum number of linkers per contact is a number  $M \geq 0$ . For  $\infty > M > 1$ , the bound linkers obey fractional statistics. In practice, the local coverage of probe molecules fluctuates [4]. We assume that the maximum number of linkers per bond, obeys Poisson statistics. Moreover, we assume that the values of  $M$  for different colloid pairs, are uncorrelated. If we average over all possible values of  $M$ , we obtain the following expression for the grand partition function of linkers (for a given  $AB$  colloidal pair):

$$Q_{AB} = \sum_{M=0}^{\infty} p(M) \sum_{L=0}^M e^{\frac{L(\mu_{AB} - \epsilon_{AB})}{T}} = \frac{1 - z e^{\overline{M}(z-1)}}{1 - z}, \quad (2)$$

where  $\overline{M}$  is the average value of  $M$ , and  $z \equiv e^{\frac{\mu_{AB} - \epsilon_{AB}}{T}}$ .  $\epsilon_{\alpha\beta}(T)$  is the temperature-dependent binding free energy of a double-stranded DNA (dsDNA) molecule connecting a given pair of  $\alpha\beta$  colloidal particles. By tuning  $\overline{M}$ , we change the effective fractional statistics of the linkers. The Bose-Einstein limit ( $Q_{AB} = 1/(1 - z)$ ) is recovered when  $\overline{M} \gg 1$ . The Fermi-Dirac limit is only recovered when  $M$  is fixed, and equal to one. The physics of DNA melting and its effect on the phase behavior of the DNA-colloid system is described exclusively by  $\epsilon_{\alpha\beta}$ .

It is straightforward to generalize the model (Eq. (1)), to the case where all three possible types of linkers are present. This results in multiplicative factors in Eq. (1) that account for all possible configurations of all linkers:  $Q_{AB}^{n_{AB}} Q_{AA}^{n_{AA}} Q_{BB}^{n_{BB}}$ , where  $Q_{AA}$  and  $Q_{BB}$  are defined analogously to  $Q_{AB}$ , Eq. (2).

The expression given by Eqs. (1, 2) can be interpreted as the partition function of a three-state spin model with Hamiltonian

$$H = \frac{1}{2} \sum_{\langle ij \rangle} \hat{\sigma}_i \hat{J} \hat{\sigma}_j - \sum_i \hat{\eta} \hat{\sigma}_i. \quad (3)$$

$\hat{\sigma}_i = (1, 0)$ ,  $(0, 1)$ , or  $(0, 0)$  if  $A$ ,  $B$ , or a vacancy (solvent) occupies site  $i$ ; and  $\hat{\eta} = (\mu_A^c, \mu_B^c)$ . The square, symmetric interaction matrix is given by  $J^{\alpha\beta} = -T \ln Q_{\alpha\beta}$ . We note that the effective attraction between the colloids induced by linkers is dominated by the entropy associated with the number of different ways of distributing  $L$  linkers over  $M$  bonds: in a dense phase, there are simply more bonds. Similar, entropic mechanisms are responsible for phase separation in binary hard-core mixtures [8], polymer-microemulsions [9], and microemulsions [10, 11].

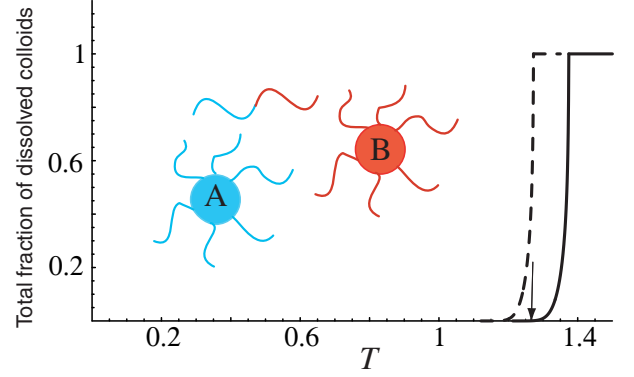


FIG. 1: Computed temperature dependence of the fraction of the ssDNA-coated colloids in the fluid (dilute) phase of a binary colloidal mixture (species  $A$  and  $B$ ) and added ssDNA linkers. Above the demixing temperature, the volume fractions of both the  $A$  and  $B$  colloids are equal to 20%. The target ssDNA can form links between  $A$  and  $B$  colloids, but not between  $A$  and  $A$ , or  $B$  and  $B$ . At low temperatures, virtually all colloids end up in the dense “gel” phase. The two curves illustrate the effect of a mutation in the target DNA. The solid and dashed curves were obtained with  $\mu \equiv \mu_{AB} = 3.5$ ,  $s = 10$ ,  $q = 6$ ,  $\overline{M} = 5$ . All temperatures are relative to the melting temperature of the perfectly complementary linker (solid curve). The dsDNA melting temperature for the dashed curve (corresponding to a base-pair mismatch) is 10 % lower than  $T_m$  for the perfectly matched linker. The arrow indicates the optimal stringency temperature.

The Hamiltonian for a three-component lattice gas model (Eq. (3)) has been studied extensively [12]. The mean-field expression for the free energy is:

$$f = T\phi_A \ln \phi_A + T\phi_B \ln \phi_B + T(1 - \phi_A - \phi_B) \ln(1 - \phi_A - \phi_B) + \frac{qJ^{AA}}{2}\phi_A^2 + \frac{qJ^{BB}}{2}\phi_B^2 + qJ^{AB}\phi_A\phi_B, \quad (4)$$

where  $\phi_A$  and  $\phi_B$  are the average volume fractions of  $A$  and  $B$  colloids. The equilibrium phase behavior of the system in the mean-field approximation follows from the analysis of this free energy [12]: depending on the strength of the interaction between the colloidal species, the system can be in a homogeneous state, or separate into two, or even three, coexisting phases. It is straightforward to generalize the model to any number of colloidal species and corresponding linkers.

We first apply the above model to analyze the experiments of Refs. [3, 4]. In those experiments, only  $AB$  linkers were present in solution, and hence  $J^{AA} = J^{BB} = 0$ . The free-energy difference between the helix and coil states of a dsDNA molecule,  $\epsilon_{AB}(T) \equiv \epsilon(T)$  constitutes an input to the interaction potential. We adopt the simple form  $\epsilon(T) = s(T - T_m)$ , where  $T_m$  is the melting temperature of a dsDNA molecule and  $s \approx 10$  [14]. The

dissolution curves of the DNA-linked colloidal aggregates are shown in Fig. 1. The fraction of colloids in solution is plotted as a function of temperature. Above a critical temperature  $T_c$ , all colloids are in solution. Consistent with the measurements of Ref. [4], the dissolution temperature of the aggregates increases with increasing surface coverage of ssDNA molecules (represented by the linker occupation number  $\overline{M}$ ) on the colloids. In the “Bose-Einstein” limit ( $\overline{M} \gg 1$ ),  $T_c$  saturates at a value  $T_c = \frac{\mu+s}{\ln[1-\exp(-8/q)]+s}$ , as follows from Eq. (4) in the case of equal initial volume fraction of colloids  $A$  and  $B$  ( $\phi_A = \phi_B$ ).

The fact that the dissolution of the DNA-linked colloidal aggregates occurs in a narrow temperature range, makes it possible to distinguish DNA strands that differ in only a single base-pair [3]. This is achieved by selecting a temperature (“optimum stringency temperature”) where a perfectly matched target results in the aggregation of a high proportion of the nanoparticles, while the same amount of ssDNA with a single mismatch causes only a small fraction of the nanoparticles to aggregate. As can be seen from Fig. 1, our model reproduces the observed behavior: For the model calculations shown in Fig. 1, the optimum stringency temperature (indicated by the arrow) is the dissolution temperature ( $T$  on the binodal) for the mismatched-DNA-linked colloids,  $T = 1.273$  (dashed curve) (in the units of  $T_m$  for the perfectly complementary dsDNA), and we assumed that  $T_m$  for the mismatched DNA is 10% lower compared with  $T_m$  of the perfectly complementary DNA. At this temperature 100% of the mismatched and only 0.1% of the perfectly complementary DNA-linked colloids are dissolved. The selectivity is thus extremely high.

Next, we consider the effect of the varying of salt concentration on the melting of the DNA-linked colloids. Added salt has two effects: It changes the DNA melting temperature and it modifies the electrostatic colloid-colloid and DNA-colloid interactions. For the salt concentrations, used in the experiments of Ref. [4], all electrostatic interactions are strongly screened [15] and hardly depend on the salt concentration. However, the salt concentration does affect the melting temperature of the DNA. To estimate this effect, we make use of the known properties of poly-electrolytes, in particular, the theoretical prediction [17] that the melting temperature of the DNA helix-coil transition is proportional to the logarithm of the salt concentration. This result has been verified experimentally (see e.g., Ref. [18]). A more detailed analysis of this result in the context of the present work will be presented in Ref. [16]. Here we simply use the fact, that for experimentally used salt concentrations, the DNA melting temperature varies with salt concentration as [13, 18]:  $T_m = T_m^0 [1 + \alpha \log c]$ , where  $T_m^0$  is the DNA melting temperature at a reference state (with a salt concentration  $I_0 = 0.1$  M),  $\alpha \approx 0.05$ , and  $c = I/I_0$ . We then obtain the following expression for  $z$ :  $z = \exp[\frac{\mu+s(1+\alpha \log c)}{T} - s]$ , where  $\mu$  and  $T$  are expressed in the units of  $T_m^0$ . This expression reproduces the ex-

perimentally observed dependence of  $T_c$  on  $\sim \log c$  [4].

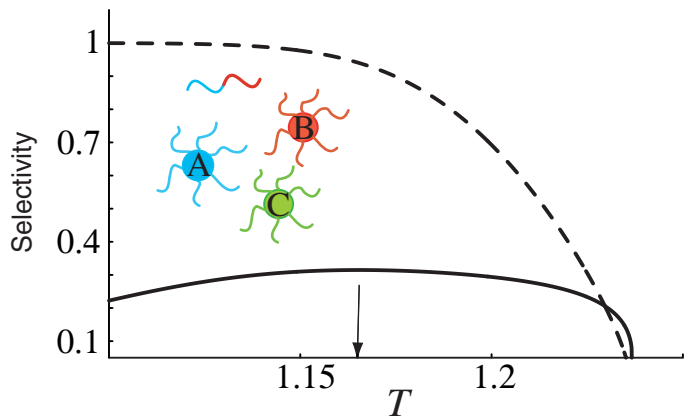


FIG. 2: Selectivity of the phase behavior of a ternary suspension consisting of  $A$ ,  $B$ , and  $C$  colloidal species and one type of ssDNA linker that is perfectly complementary to  $AB$  pair and slightly mismatched with respect to  $AC$  pair (see text). The solid (dashed) curves show that the presence of  $AB$  linkers induces a large relative concentration differences  $(\phi_B - \phi_C)/(\phi_B + \phi_C)$  of  $B$  and  $C$  colloidal species in the dense (solid curve) and dilute  $-(\phi_B - \phi_C)/(\phi_B + \phi_C)$  (dashed curve) phases, respectively. Above the demixing temperature, the concentration of all colloidal species is the same:  $\phi_A = \phi_B = \phi_C = 0.17$ . The parameters used in to compute this figure are:  $\mu = 2.5$ ,  $s = 10$ ,  $q = 6$ ,  $\overline{M} = 3$ .  $T$  and  $\mu$  are expressed in the units of  $T_m$  of the linker that binds  $AB$ . The melting temperature of the linker connecting  $AC$  was assumed to be only 5% lower than  $T_m$ . The arrow indicates the optimal stringency temperature.

The model described above suggests a novel approach to DNA screening (mutation analysis). As mentioned above, colloids functionalized with oligonucleotides have been used as probes to differentiate perfectly complementary targets from those with single-base mismatches (see Ref. [3]). The drawback of the existing method is that the thermodynamic properties of DNA-linked nanoparticle assemblies are sensitive to the parameters of the system, such as the grafting DNA density, the concentrations of DNA linkers and colloids, the monodispersity of colloids, and the pH and ionic strength of the solvent. As it is essential to maintain precisely the same experimental conditions when performing the measurements on different target DNA strands, mutation-screening experiments are rather demanding.

Here we propose a method that should be relatively insensitive to unavoidable variations in the experimental conditions. To illustrate our approach, consider a system consisting of three colloidal species  $A$ ,  $B$ , and  $C$  (see Fig. 2). Species  $B$  and  $C$  are grafted with ssDNA molecules that have similar sequences and only different by a mismatch (either a single-base or multiple-base). We assume that the target ssDNA is either perfectly complementary to  $AB$  sequence, or mutated, and thus perfectly

complementary to  $AC$  sequence (the method is easily generalized to a larger possible number of mutations).

The addition of the target ssDNA, induces a two-phase separation in the system. Importantly, the composition of the dense aggregate (and, by implication, the composition of the remaining solution) depends on the nature of the target ssDNA. The characteristic mean-field phase diagram for this case is shown in Fig. 2 in terms of the concentration differences (selectivity plot) between  $B$  and  $C$  colloids. The target is perfectly complementary to  $AB$ . The melting temperature of the target DNA is assumed to be some 5% higher for a perfectly matched sequence than for a mismatched sequence. The initial concentrations of  $A$ ,  $B$ , and  $C$  colloids are chosen to be equal. Our main prediction is that the sequence of the target can be determined simply by monitoring the concentration *differences* of the species  $B$  and  $C$  in either a dense (solid curve) or dilute (dashed curve) phase. In the case shown in Fig. 2, at the optimal stringency temperature  $T \approx 1.165$  (in the units of  $T_m$  of the  $AB$  linker), the difference between the concentrations of  $B$  and  $C$  colloids

in the aggregated phase is as large as 30%. If the colloids fluorescently labeled, even small differences in concentrations can easily be detected. In this way, a single experiment allows us to distinguish between the perfectly complementary and mismatched target. We stress that the selectivity of the DNA screening can be tuned by varying the surface coverage density  $\overline{M}$ . The method should be robust to moderate variations in the experimental conditions. It is straightforward to generalize the technique to discriminate between a larger number of possible mutations, simply by increasing the number of colloidal probe species.

In essence, the method allows us to map the microscopic base-pair sequence of the target ssDNA onto the macroscopic phase behavior of the DNA-linked nanoparticle solution.

We are grateful to W.C. Poon, T. Schilling, A. Cacciuto and S. Tans for helpful comments. The work of the FOM Institute is part of the research program of FOM and is made possible by financial support from the Netherlands organization for Scientific Research (NWO).

- 
- [1] N. C. Seeman, *Nature*, **421**, 427 (2003).
  - [2] C. A. Mirkin et al., *Nature*, **382**, 607 (1996).
  - [3] T. A. Taton, C. A. Mirkin, R. L. Letsinger, *Science*, **289**, 1757 (2000).
  - [4] R. Jin, G. Wu, Z. Li, C. A. Mirkin, and G. C. Schatz, *JACS*, **125**, 1643 (2003).
  - [5] C.-H. Kiang, *Physica A*, **321**, 164 (2003).
  - [6] In Refs. [3, 4], the word “melting” is used to describe the process of dissolution of the DNA-linked colloidal aggregates. In the present work, we avoid the use of terms “melting” and “freezing” for this transition and use instead “dissolution” and “demixing”, as we argue that it is, in fact, more closely related to a liquid-liquid phase separation. This phase transition should also be distinguished from the melting of ssDNA linker molecules bound to complementary ssDNA grafted to colloids.
  - [7] At this level of description, we ignore the interaction between different linkers.
  - [8] D. Frenkel and A. A. Louis, *Phys. Rev. Lett.*, **68**, 3363 (1992).
  - [9] A. Zilman, J. Kieffer, F. Molino, G. Porte, and S.A. Safran, *Phys. Rev. Lett.*, **91**, 015901 (2003).
  - [10] T. Drye and M. E. Cates, *J. Chem. Phys.*, **96**, 1367 (1992).
  - [11] T. Tlusty, S. A. Safran, and R. Strey, *Phys. Rev. Lett.*, **84**, 1244 (2000).
  - [12] S. Krinsky and D. Mukamel, *Phys. Rev. B*, **11**, 399 (1975); D. Furman, S. Dattagupta, and R. B. Griffiths, *Phys. Rev. B*, **15**, 441 (1977); T. Schilling and G. Gompfer, *J. Chem. Phys.*, **117**, 7284 (2002).
  - [13] I. Rouzina and V. A. Bloomfield, *Biophys. J.*, **77**, 3242 (1999).
  - [14] The expression for the free energy difference that we employ ( $\epsilon(T) = s(T - T_m)$ , where  $s \sim N|\Delta S|$ ), represents the first term in the expansion of the exact free energy,  $\epsilon(T) \sim N(\Delta H - T\Delta S)$ , where  $N$  is the number of base pairs in a DNA molecule,  $\Delta H$  and  $\Delta S$  are, respectively, the enthalpy and entropy difference between the helix and coil states at a given temperature per base pair (see e.g. Ref. [13]).
  - [15] We note that in experiments [4], the salt concentration varied in the range  $\sim 0.1\text{M} - 1\text{M}$ . This corresponds to the Debye screening radius of  $\sim 1\text{nm} - 0.3\text{nm}$ , respectively, which is at least one order of magnitude *smaller* than the size of colloids and length of DNA linkers. The *direct* electrostatic interaction between the colloids in solution is thus effectively screened. However, at lower salt concentrations, direct electrostatic effects may become significant. This phenomenon will be discussed in Ref. [16].
  - [16] D. B. Lukatsky and D. Frenkel (to be published).
  - [17] G. C. Manning, *Biopolymers* **15**, 1333 (1975); M. D. Frank-Kamenetskii, V. V. Anshelevich, and A. V. Lukashin, *Sov. Phys. Uspekhi*, **151**, 595 (1987); J. Bond, C. Anderson, and M. T. Record, *Biophys. J.*, **67**, 825 (1994).
  - [18] R. D. Blake and S. G. Delcourt, *Nucleic Acids Res.*, **26**, 3323 (1998).